ELSEVIER

Journal of Power Sources 90 (2000) 182–187

JOURNAL OF POWER SOURCES

www.elsevier.com/locate/jpowsour

Anodic oxidation behaviour of aluminium in propylene carbonate

Jin Kawakita*, Kenzo Kobayashi

Department of Chemistry, Faculty of Science and Technology, Keio University, Hiyoshi 3-14-1, Kohoku-ku, Yokohama 223-8522, Japan

Received 17 August 1999; received in revised form 11 January 2000; accepted 19 February 2000

Abstract

The anodic oxidation behaviour of pure aluminium (Al) in propylene carbonate was investigated using electrochemical measurements, microscopic observations, elemental and gravimetric analyses. The formation and growth of the oxide were observed on the surface of Al in the early stage of anodizing. Further anodic oxidation led to the breakdown of a part of the oxide film, resulting in simultaneous pitting corrosion because of the limitation of mass transfer in the oxide layer. © 2000 Elsevier Science S.A. All rights reserved.

Keywords: Aluminium; Anodizing; Surface oxide; Corrosion; FE-SEM; EQCM

1. Introduction

The electric vehicles require power sources with higher power density, rapid rechargeability, and long cycle life. Lithium and lithium ion secondary batteries are their candidates, which are able to respond to these requirements. In secondary battery, oxidation and reduction reactions proceed at the positive electrode during charge and discharge processes, respectively. Lithium and lithium ion cells have main reactions, which are extraction and insertion of lithium ion (Li^+) from and into the electrode active materials, e.g. $LiCoO_2$, in the electrolyte composed of a mixture of a non-aqueous solvent and lithium salt. These reactions occur at the potential above 4.0 V vs. Li/Li^+ standard one.

To exchange electrons between active material and external circuit in cells, the electrode possesses a conductive substance called the current collector. When the cell is charged, the current collector of the positive electrode has a high potential above 4.0 V close to the active material because the former contacts with the latter. In such a high potential, i.e. under highly oxidative condition, corrosion of most metals is inevitable. In general, however, aluminium (Al) is corrosion-resistant in air and neutral in water environments without aggressive materials, because the surface of Al itself is covered with a protective oxide film. This character was expected to be retained to some extent even in the non-aqueous electrolyte. Therefore, in a commercial lithium ion battery, Al has been used for the positive electrode as a current collector.

The electrochemical oxidation behaviour of Al in a non-aqueous electrolyte has been investigated by many authors. The results were classified mainly into three phenomena: (i) pitting corrosion of Al, i.e. localized change of metal to dissolved cation [1–5]; (ii) formation of a passive film or layer [6–9]; and (iii) decomposition of the electrolyte [10,11] on the surface of the Al electrode. Furthermore, it has been reported that the aluminium current collector was also corroded in the battery system using polymer electrolytes [12,13].

In this study, in order to elucidate the reaction mechanism of the phenomenon taking place on the current collector of the positive electrode during charging of the lithium ion cell, the anodic oxidation behaviour of Al in the lithium perchlorate/propylene carbonate ($LiClO_4$/PC) solution was investigated using polarization measurement, electrochemical quartz crystal microbalance (EQCM), field emission scanning electron microscopy (FE-SEM), and X-ray photoelectron spectroscopy (XPS). These are gravimetry connected with electrochemical measurement,

* Corresponding author. National Research Institute for Metals, 1-2-1, Sengen, Tsukuba-shi, Ibaraki-ken 305-0047, Japan. Tel.: +81-298-59-2124; fax: +81-298-59-2101.

E-mail address: kawakita@nrim.go.jp (J. Kawakita).

PII: S0378-7753(00)00408-0

microscopic observation of the surface and the cross-section, and elemental analysis of the Al surface state.

2. Experimental

Specimens of Al (Wako; 4 N in purity) were cut into small pieces with dimensions of $10 \times 40 \times 0.2$ mm^3, and degreased by sonication in acetone for 30 min and dried in a cool air stream.

The specimens of Al were electropolished at an anodic constant current density of 100 mA cm^{-2} in a mixed solution of perchloric acid and ethanol (= 1:4 in volume ratio) below 10°C for around 3 min to obtain a mirror-like surface. Immediately after the electropolishing, the specimens were immersed into and washed thoroughly in absolute ethanol. Finally, the specimens were dried in a cool air stream.

Electrochemical measurements were carried out in a cylindrical glass cell with the three electrodes. An electropolished specimen of Al and a foil of Al were used as the working and the counter electrodes, respectively. The reference electrode was a metallic lithium rod (Aldrich; 3.2 mm in diameter), which was embedded in a glass tube with a glass–wool membrane at one end and filled with the electrolyte. The PC solution containing 1 mol dm^{-3} $LiClO_4$ (Mitsubishi Chemical; water content < 20 ppm) was adopted as the electrolyte. Anodic oxidation was performed by two methods. There were galvanostatic oxidation at anodic current densities of 0.01–5.0 mA cm^{-2}, and anodic potential sweep at a scan rate of 50 mV s^{-1} from the rest potential to 10 V with an aid of a galvanostat/potentiostat (Hokuto Denko; HA-301) connected with a function generator (Hokuto Denko; HB-104). All the procedures were conducted in a glove box filled with argon gas. In this paper, the electrode potential is described as volt vs. Li/Li$^+$.

The surface and the cross-section of the specimen before and after anodic oxidation were observed by FE-SEM (Hitachi S-4700). For the observation of the cross-section, a specimen was embedded into epoxy resin in a capsule, and was sharpened and trimmed at an end with a glass knife followed by a diamond to expose the cross-section by removal of the resin.

The surface of the Al specimen was characterized by XPS using a JEOL apparatus (JPS-9000MC) with an Mg Kα anode X-ray source with primary beam energy of 15 kV and an electron current of 20 mA.

The weight change of the specimen during anodic oxidation was determined using EQCM of Hokuto Denko HQ-302. The working electrode was prepared by evaporation of Al on an AT cut quartz disc by RF sputtering with a target metal of Al (4 N, Furuuchi Chemical) under a trace of argon gas. The original resonance frequency of the quartz is 6 MHz. The evaporated Al film had the geometric surface area of 1.327 cm^2 and the thickness of approximately some hundred nanometers, which was calculated by the average accumulation rate (400 nm min^{-1}). Except for the working electrode, the EQCM experiment was carried out using the same component parts of the electrochemical cell as described above.

3. Results and discussion

The anodic polarization curve of an Al specimen at 50 mV s^{-1} is shown in Fig. 1. The current begins to flow at 3.5 V (vs. Li/Li$^+$) and increases gradually until the potential reaches about 5.0 V. Then, the current keeps almost constant value of 5 μA cm^{-2}, indicating that the reaction rate is limited by the mass transfer. From this result, the formation of the solid-state film might take place on the electrode surface rather than decomposition of the electrolyte in the potential ranges over 3.5 V.

The typical galvanostatic oxidation behaviour at 0.3 mA cm^{-2} as a function of time is shown in Fig. 2. The potential vs. time curves at constant applied current densities between 0.01 and 5.0 mA cm^{-2} showed almost the same tendency while their slopes up to attainment of the fluctuating potential and the values of the fluctuating potential depended on the applied current densities. After the circuit is closed, the electrode potential rises because of the resistance of an air-formed oxide film on the Al surface. The consecutive increase in the potential up to about 25 V can be considered as corresponding to growth (or expansion) of the oxide layer as discussed later. The fluctuating potential around 25 V is explained by localized breakdown and repassivation of the oxide film on the Al surface, as observed in the excessive anodic oxidation of Al in the neutral aqueous solution. Considerably high potential of 25 V may cause decomposition of the electrolyte in competition with the breakdown. As soon as the

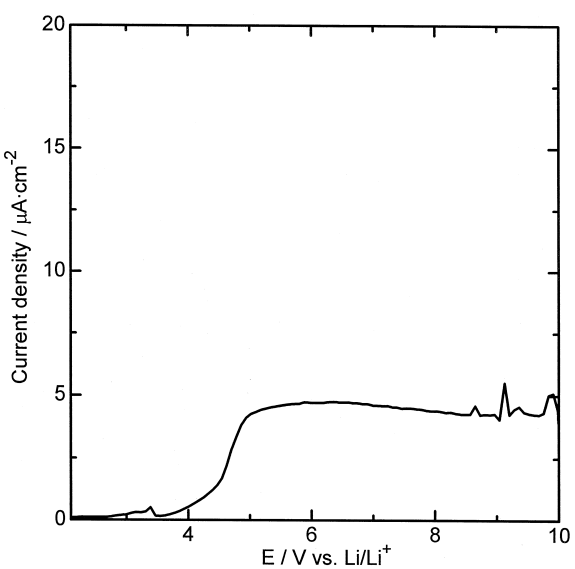

Fig. 1. Polarization curve of Al electrode at 50 mV s^{-1}.

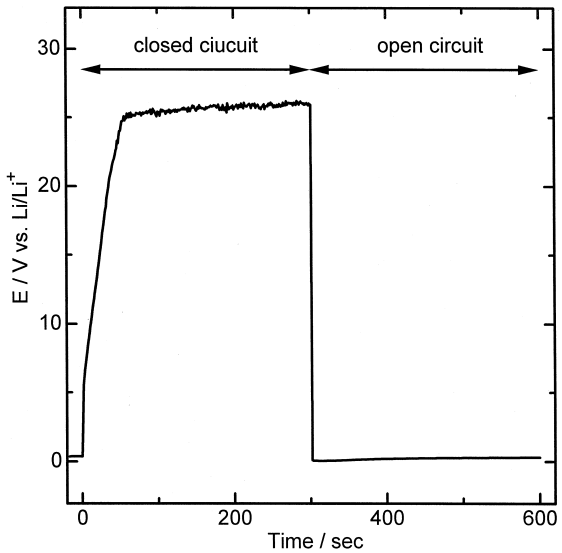

Fig. 2. Potential of Al electrode as a function of oxidation time at +0.3 mA cm^{-2}.

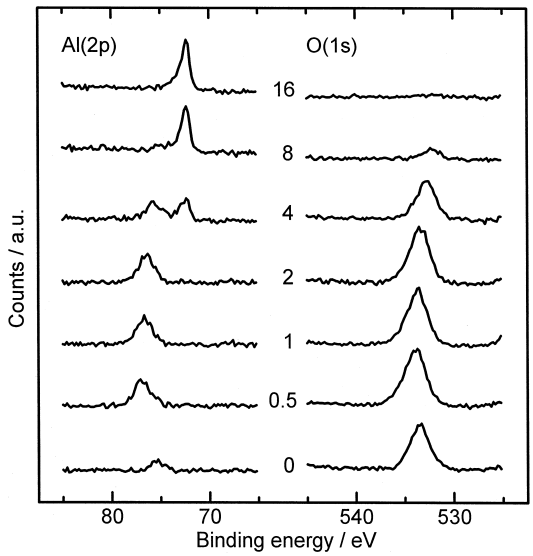

Fig. 4. XPS spectra of Al(2p) and O(1s) for Al specimen anodized at +50 μA cm^{-2} up to 20 V.

applied current is off, the electrode potential is dropped rapidly near the rest potential of the Al specimen before the anodic oxidation, and then increases slightly. This phenomenon is explained by the reason that the broken passive oxide film is gradually repaired over the Al substrate. In a practical use, however, the breakdown would not be realized on charging of batteries because the upper limit of the potential at the positive electrode is restricted to be 5.0 V, at most.

The XPS spectra obtained from the Al surface electropolished, anodized at 50 μA cm^{-2} and 5.0 mA cm^{-2} are shown in Figs. 3–5, respectively. Peaks in the left-and right-hand side of spectra in the figures are ascribed to electrons situated in Al(2p) and O(1s) energy levels, respectively. The uppermost spectra in the respective figure describe the specimen subjected to etching with Ar^+ ion for the sufficiently long period. Figures on the curves indicate the accumulated time of etching. As shown in Fig. 3, peaks near 76, 72 and 534 eV before etching are attributed to the energy levels of Al^{3+}, Al^0, and O^{2-} constituents, respectively, indicating the presence of a large amount of oxides mainly consisting of Al_2O_3 and a little bit of metallic Al at the innermost surface of the specimen. As etching time increases, peaks assigned to Al^{3+} and O^{2-} constituents become weaker and eventually disappear after 4 min of etching. Therefore, it is considered that the electropolished Al sample is covered with oxides of Al_2O_3 in thickness corresponding to etching time of 4 min. Fig. 4 shows the spectra of Al specimen

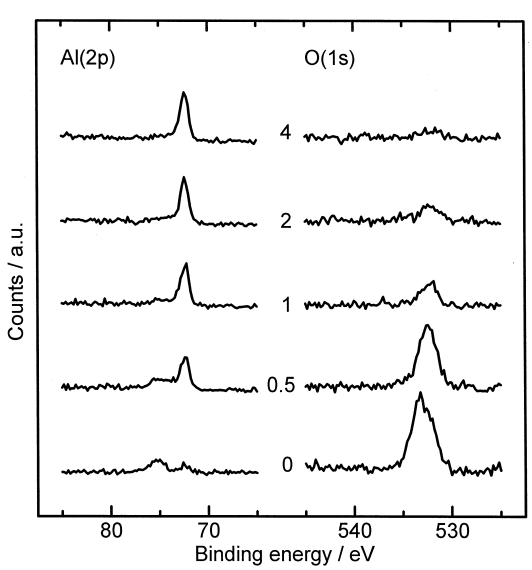

Fig. 3. XPS spectra of Al(2p) and O(1s) for electropolished Al specimen.

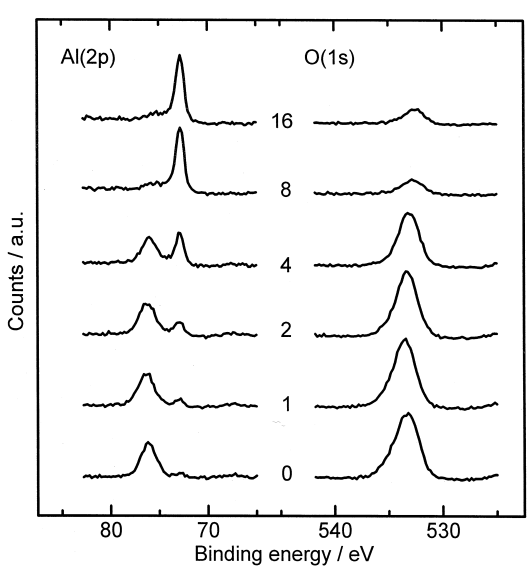

Fig. 5. XPS spectra of Al(2p) and O(1s) for Al specimen anodized at +5.0 mA cm^{-2} for 5 min.

anodized at 50 μA cm^{-2} up to 20 V, just before reaching the fluctuant potential, as shown in Fig. 2. Although the etching time was prolonged, peaks attributed to Al^{3+} and O^{2-} constituents were clearly retained and no peaks were observed regarding the Al^{0} levels. Obvious peaks are observed in Al^{3+} and O^{2-} levels even after Ar^{+} ion etching for 4 min. In addition, no chlorine (Cl) element was detected by XPS measurement. From these results, the growth of the oxide layer can be considered to take place quickly in the early stage of anodic oxidation. Furthermore, the spectra of the Al specimen anodized highly at 5.0 mA cm^{-2} for 5 min are shown in Fig. 5. The potential with fluctuation was kept at about 27 V almost throughout anodization. The surface had a lot of visible pitting. At 8 min etching, a peak ascribed to the Al^{3+} constituent can be seen to become much weaker than that at shorter etching times, while the O^{2-} peak exists and is still observed after 16 min. Accordingly, it can be considered that the whole Al surface was covered with the oxide layer, having a certain extent of thickness, and thin oxide layer on the pitting sites, where the breakdown took place.

Microscopic observation explains well the corrosion processes of the Al specimen during anodic oxidation. The SEM images of Al surface anodized at 0.3 mA cm^{-2}, and 5.0 mA cm^{-2} are shown in Figs. 6 and 7, respectively. A small hole or pit is clearly observed in the middle, as seen in Fig. 6a. The breakdown can be presumed to occur at a defect on the oxide surface, resulting in the hole. The magnified hole is shown in Fig. 6b. The steps can be observed inside the hole, suggesting that elution develops inward the Al substrate. As a higher electric current flew in a small area like the hole, the further elution reaction proceeded, as shown in Fig. 7a. The hole-like dimple having steps can be seen in Fig. 7b. The cross-sectional SEM images of the Al specimen anodized at 0.3 and 5.0 mA cm^{-2} are presented in Figs. 8 and 9. At the moderately anodized surface, there are small pits perpendicular to the interface between the substrate and the epoxy resin, as seen in Fig. 8a. In the magnified profile of a pit, as shown in Fig. 8b, a dimple can be observed to have steps similar to the one observed in the plan-view as shown in Fig. 6b. For the highly anodized Al specimen, there are huge pits, which seemed to consist of a number of overlapped dimples, as shown in Fig. 9a. The step profile is confirmed also by its magnified part, as seen in Fig. 9b. From the SEM observations, the elution mechanism will be able to assume as follows. As soon as the rate of the mass transfer in the oxide becomes smaller than the current through it, the growth of the oxide layer stops, and alternatively, the breakdown begins to take place at the interface between

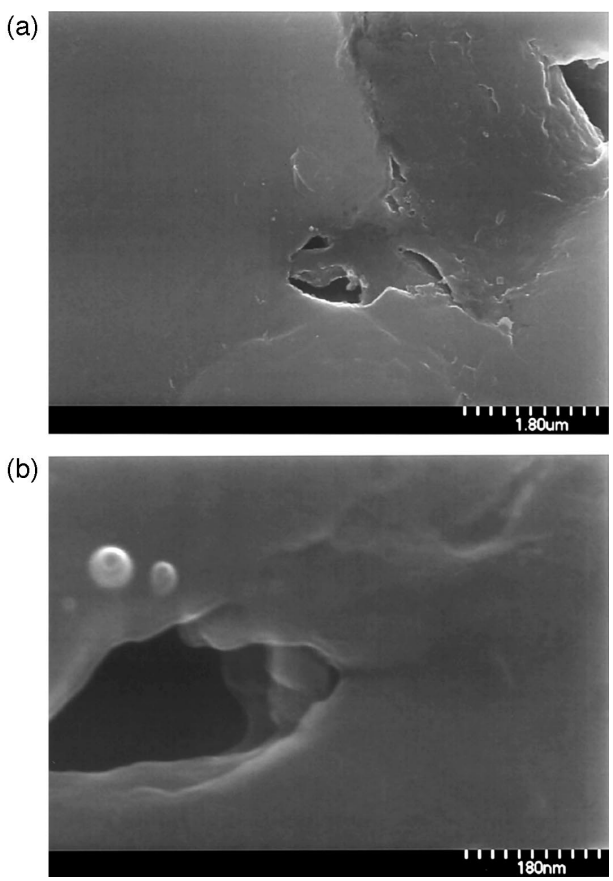

Fig. 6. SEM images of surface of Al specimen anodized at +0.3 mA cm^{-2}: (a) ×10,000; (b) ×100,000.

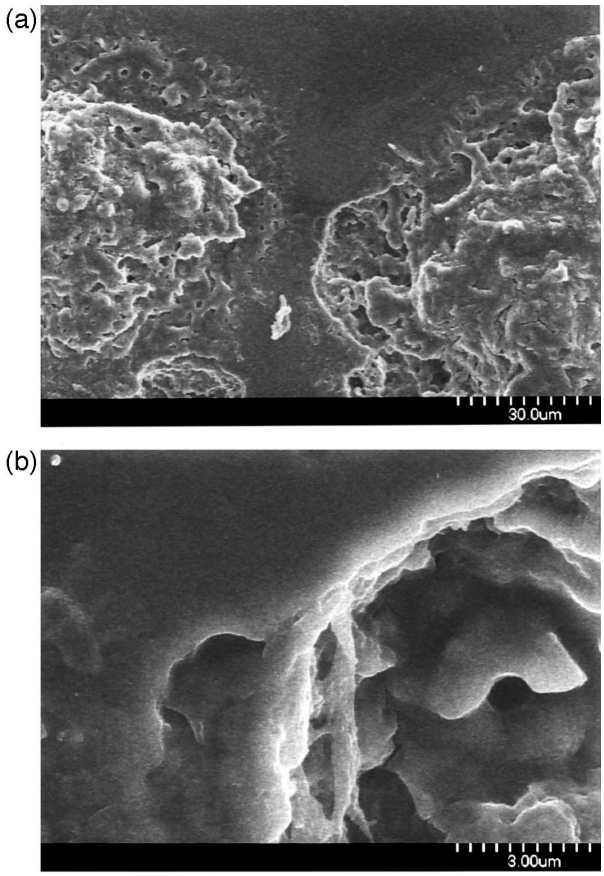

Fig. 7. SEM images of surface of Al specimen anodized at +5.0 mA cm^{-2}: (a) ×1000; (b) ×10,000.

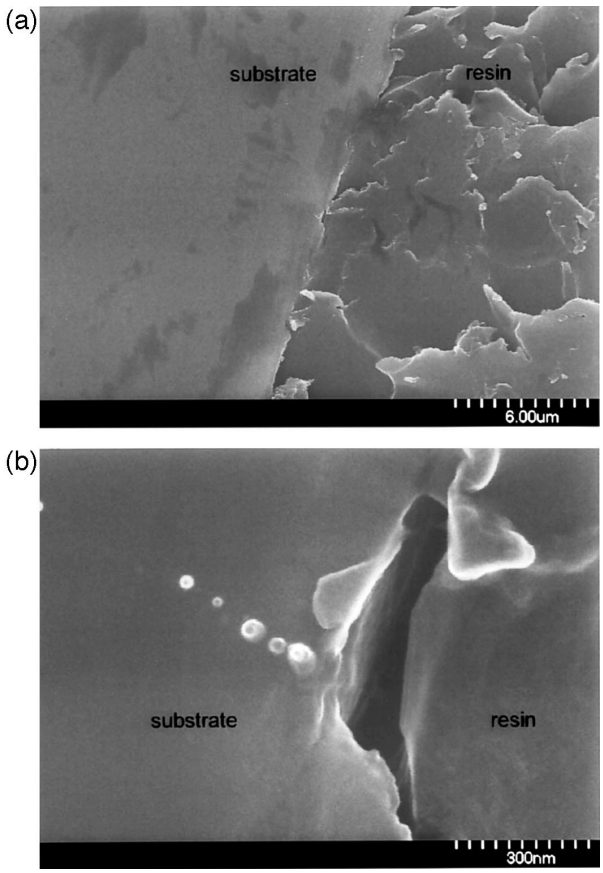

Fig. 8. SEM images of cross-section of Al specimen anodized at +0.3 mA cm^{-2}: (a) ×5000; (b) ×100,000.

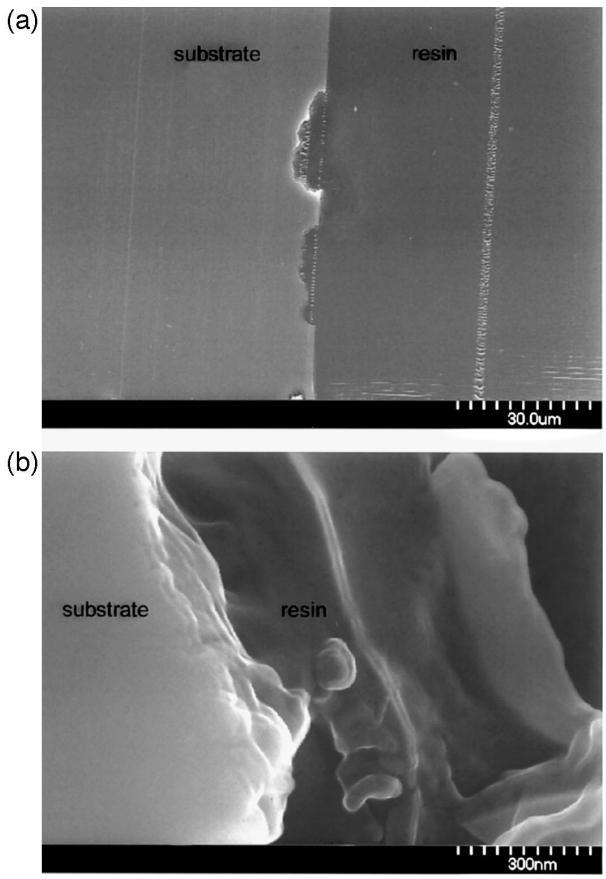

Fig. 9. SEM images of cross-section of Al specimen anodized at +5.0 mA cm^{-2}: (a) ×1000; (b) ×10,000.

the Al substrate and the oxide. At this site, the current density for the elution process is considerably large and exceeds the formation rate of the oxide, because the rest of the Al substrate is still covered with a poorly conductive oxide film. Furthermore, the rapid increase in the concentration of cation around this site, i.e. in the bottom of the oxide layer, ceases to advance the elution toward the depth direction. Accordingly, the elution process prefers the horizontal direction to the vertical one, and the remaining profile looks like a dimple or a mortar.

A typical result of EQCM measurement is shown in Fig. 10. Originally, QCM gives a steady resonance frequency of the quartz crystal on the fine AC voltage impression, and the mass changes on the surface, such as adsorption, or dissolution, etc. are represented as the changes of the resonance frequency. Fig. 10a shows the variation of the resonance frequency (Δf) as a function of time during galvanostatic anodic oxidation at +0.3 mA cm^{-2} where the potential is kept at the steady state. A linear increase in Δf is caused by a decrease in weight together with the removal of Al element from the electrode during oxidation. The frequency change is converted to weight (Δw) by using the equation proposed by Sauerbrey [14], and is presented as the solid line in Fig. 10b. The dotted line shows the value obtained by calculation according to Faraday's law, assuming that the whole electric

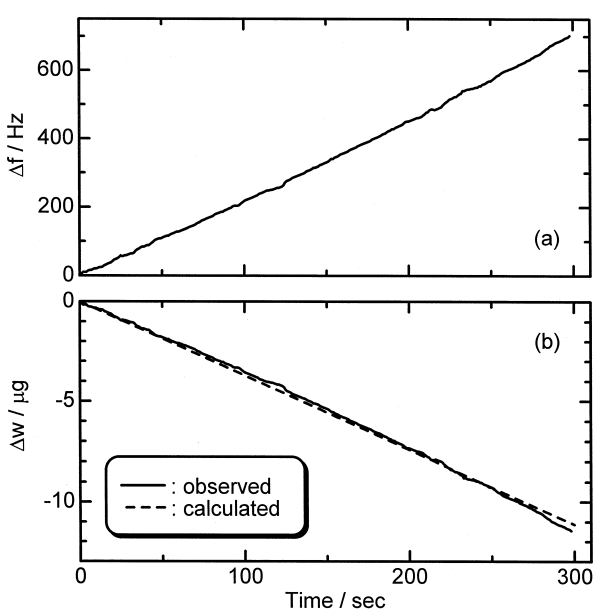

Fig. 10. Frequency (a, upper) and weight changes (b, lower) of Al electrode vs. time in potential fluctuating region during anodization.

current is consumed for the elution of Al from the electrode in the following equation:

$$Al \rightarrow Al^{3+} + 3e^{-}.$$

The solid line consistent with calculated one indicates that anodic oxidation of Al in $LiClO_4$/PC causes changing of Al^0 metal to Al^{3+} ion. Note that the potential during EQCM measurement reached the steady value immediately after the circuit was closed and it was kept at about 3.6 V. Probably, the decomposition of the electrolyte is considered not to take place on the electrode surface, because of the stability of the electrolyte at this potential [3]. In addition, a plateau of the potential indicates that the less conductive oxide was not formed. The potential of 3.6 V in the EQCM measurement is considerably lower than that in the electrochemical measurement as shown in Fig. 2. This phenomenon can be explained by the difference in the surface condition between the electrodes used in both experiments. The electropolished specimen for the electrochemical measurement has a smooth plane composed of the large crystal grain. On the other hand, the surface of the specimen for the EQCM measurement is considerably rough and formed by aggregation of small particles when the EQCM sample was prepared by evaporation of Al on the quartz crystal disc. Compared with the electropolished specimen, the EQCM sample has a larger actual surface area with more defects and so the elution of the Al element is feasible to take place rather than the steady growth of the oxide layer at the surface. Accordingly, the result of EQCM shows that the whole current was consumed for the elution and not for the side reaction such as decomposition of the electrolyte and formation of the oxide.

4. Conclusion

The anodic oxidation of pure aluminium proceeded in two steps. Firstly, the oxide film formed and grew on the Al substrate. When the rate of mass transfer in the oxide reached the critical point, part of the oxide layer was broken down at the interface between the oxide and the substrate, where exposed Al^0 metal was directly oxidized to Al^{3+} ion to dissolve into the solution.

Localized elution of the Al element left dimples at the surface, as oxidation proceeded. At the site of the breakdown, considerably high current was flowed and high concentration of Al^{3+} ion determined the elution direction to horizontally in preference to perpendicularly, leading to production of corroded pores with the hemispherical shape.

References

[1] K.V. Rybalka, L.A. Beketaeva, J. Power Sources 42 (1993) 377.
[2] L.J. Krause, W. Lamanna, J. Summerfield, M. Engle, G. Korba, R. Loch, R. Atanasoski, J. Power Sources 68 (1997) 320.
[3] P. Arona, R.E. White, M. Doyle, J. Electrochem. Soc. 145 (1998) 3647.
[4] K.V. Rybalka, L.A. Beketaeva, Russ. J. Electrochem. 34 (1998) 1262.
[5] J.W. Braithwaite, A. Gonzales, G. Nagasubramanian, S.J. Lucero, D.E. Peebles, J.A. Ohlhausen, W.R. Cieslak, J. Electrochem. Soc. 146 (1999) 448.
[6] K. Wang, P.N. Ross Jr., Surf. Sci. 365 (1996) 753.
[7] M. Morita, Y. Matsuda, J. Power Sources 60 (1996) 179.
[8] M. Ue, F. Mizutani, S. Takeuchi, N. Sato, J. Electrochem. Soc. 144 (1997) 3743.
[9] W.K. Behl, E.J. Plichta, J. Power Sources 72 (1998) 132.
[10] K. Kanamura, S. Toriyama, S. Shiraishi, Z. Takehara, J. Electrochem. Soc. 142 (1995) 1383.
[11] K. Kanamura, T. Ogiwara, Z. Takehara, J. Power Sources 57 (1995) 119.
[12] H.S. Choe, B.G. Carroll, D.M. Pasquaiello, K.M. Abraham, Chem. Mater. 9 (1997) 369.
[13] Y. Chen, T.M. Devine, J.W. Evans, O.R. Monteiro, I.G. Brown, J. Electrochem. Soc. 146 (1999) 1310.
[14] G. Sauerbrey, Z. Phyz. 155 (1959) 206.